Morphing Tank-to-Leg Modality for Exploratory Lunar Vehicles

University of Connecticut
Connecticut Space Grant Consortium

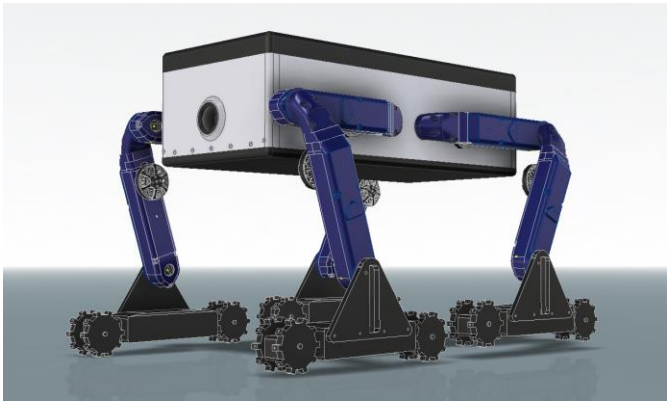

Jenna Abbruzzese: Undergraduate in Marketing
Michael Aisevbonaye: Undergraduate in Mechanical Engineering
Aditya Awasthi: Undergraduate in Mechanical Engineering, Minor in Mathematics
Jonathan Bane: Undergraduate in Materials Science and Engineering
Hritish Bhargava: Undergraduate in Engineering Physics
Jamison Cote: Undergraduate in Digital Media and Design, Minor in Entrepreneurship and Tech Innovation
Alaa Emad El Din: PhD candidate in Electrical & Computer Engineering – foreign national student
Abhiram Gunti: Undergraduate Computer Science, Minor in Mathematics
Grayson Hall: Undergraduate in Mechanical Engineering, Minor in Computer Science
Rany Kamel: Undergraduate in Computer Science & Engineering, Minor in Mathematics
Jiovanni Kissi: Undergraduate in Mechanical Engineering Concentration in Aerospace, Minor in Astrophysics
Kalin Kochnev: Undergraduate in Computer Science and Engineering
Christina Lawrence: Undergraduate in Chemical Engineering and Molecular and Cell Biology
Theresa Nosel: Undergraduate in Chemical Engineering and Materials Science and Engineering
Blake Pember: Undergraduate in Computer Engineering
Sana Qureshi: Undergraduate in Applied Mathematics and Material Science and Engineering
Emily Rondeau: Undergraduate in Materials Science and Engineering
Vihaan Shah: Undergraduate in Computer Science, Minor in Mathematics
Matt Silverman: Undergraduate in Electrical Engineering, Minor in Computer Science
Elliott Trester: Undergraduate in Materials Science and Engineering, Minor in Mathematics
Sabrina Uva: PhD Student in Human Development and Family Sciences
Anna Vladimirskaya: Undergraduate in Computer Science and Robotics Engineering

Dr. Fiona Leek: Department of Materials Science and Engineering University of Connecticut
Dr. Ramesh Malla: Department of Civil and Environmental Engineering University of Connecticut

Table of Contents

1.0 Quad Chart

Morphing Tank-to-Leg Modality for Exploratory Lunar Vehicles
University of Connecticut

Concept Synopsis

Goal: Engineer a modality to be utilized on the lunar south pole.
Technical Approach: A morphing tank-to leg modality
Objectives:
1. Refine design to optimize mechanical function of modality
2. Program the morphing modality
3. Traverse sloped surfaces up to 36°
4. Traverse icy landscapes

With the conclusion of the challenge, this team has fully designed the prototype and are in the process of manufacturing and assembling all components

Image Depicting Concept

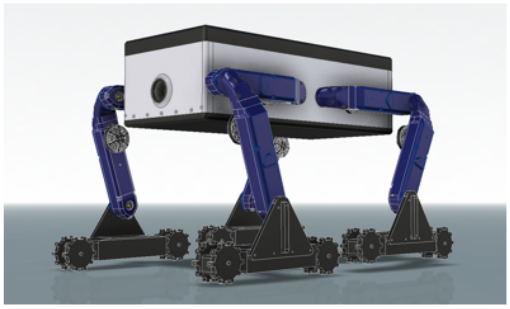

Innovations

The lunar south pole is expected to have slopes around and in craters of up to 36° and icy regolith at the base of those craters. Current technology has difficulty navigating such a diverse terrain. The combination of two modalities into one morphing one is being done to combine the following advantages:

- Tank: Robust stability, traction, energy efficiency
- Quadruped: Adaptable stability, inclines

This is be custom designed by the team to prove the capability of such a union.

Verification Testing Results & Conclusions

Verification Testing:
1. Testing of the programming to hardware connectivity has been successful. The programming of tank and preliminary quadruped motions have also successfully been done using a single appendage. 2. Testing with four appendages and in predetermined environments will occur in the future

Conclusions:
This team believes in the viability of using a morphing modality approach to the defined terrain. More time is needed to develop and test the prototype, which the team will continue to do after the conclusion of this challenge.

2.0 Executive Summary

The Moon is a staging ground for exploring the rest of space. The accessibility to ice and solar power makes the south pole an area of interest for scientists[1]. Ice offers oxygen to breathe and water to drink, and both are key to sustaining a long-term human presence on the moon. There is also potential in using hydrogen and oxygen as a source of rocket fuel[2]. South pole highlands offer an ideal location for utilizing solar power.

Traversing the lunar south pole is particularly challenging as it is defined by harsh topography and deep craters. The highlands and lowlands are separated by steep slopes, most under 40° but some as steep as 80.21°[3]. As such, future Lunar Exploration Vehicles will require the ability to traverse 30° to 40° slopes within icy operating conditions in temperatures as low as -243°C. Slopes greater than 30° and icy lunar regolith are not traversable by current rovers.

To allow rover mobility in this harsh, currently inaccessible lunar terrain, this team developed a morphing tank-to-leg modality with configurations designed to overcome the challenges stated above. The product is titled Adaptive Morphing and Balanced Exploratory Rover (AMBER). This morphing modality involves four appendages capable of functioning as a quadruped (Figure 2.1), a tank (Figure 2.2), or combination of the two (Figure 2.3). The combination of tank and legs is used for obstacle avoidance and increased stability. The up-and-down stepping movement of the leg allows for improved motion through ice.

Figure 2.1 “Leg/Quadruped-mode”

Figure 2.2 “Tank-mode”

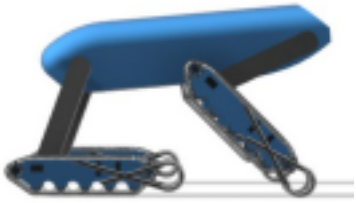

Figure 2.3 “Combination mode”

This morphing modality design will be tested in the future against lunar-simulated environmental conditions. This will include a miniature slope lab (MSL) filled with sand and eventually mid-sized rocks. A hinge mechanism will allow the test slope to be adjusted to various angles between 10° and 36°. The MSL will allow for qualitative analysis of the modality’s ability to travel up and down steep slopes. To determine the morphing modality’s capabilities in icy conditions, testing will take place on a flat, icy surface (hockey rink), as well as in a chest freezer of frozen LHS-1 lunar simulant soil. Additional testing will occur in high vacuum and cryogenic environments to simulate the atmospheric conditions of the Moon.

The adaptability of the morphing design makes it possible for the modality to traverse a more diverse terrain than is possible with a singular, conventional modality. Thus, this morphing modality design enables exploration of lunar regions that have been previously inaccessible and “help NASA go forward to the Moon.”

3.0 Problem Statement and Background

3.1 Problem Statement

The goal of this project is to design a novel locomotion modality for NASA’s autonomous lunar rover to tackle the unique challenges posed by the complex environment found at the lunar south pole. The focus is on overcoming the challenges associated with the traversal of steep slopes and icy surfaces. The modality will have to traverse terrain up to 36° to successfully ascend and descend crater walls found around the lunar south pole[4]. Within craters, the modality will have to maneuver through icy patches and endure

temperatures as low as -243°C[4]. The modality must prove itself dependable, effective, and efficient in functionality and particulate contamination prevention and mitigation.

3.2 Background

Historically, NASA and its international counterparts utilized a wide variety of wheel and suspension combinations for off-world use. As missions have moved to Mars, six-wheeled rovers with a rocker-bogie suspension have become the predominant design to traverse the mostly flat Martian terrain[5]. This suspension design equally distributes weight to all six wheels to minimize slip and tilt, but at the cost of limiting the rover to slopes less than 30°. While an improvement over the ~20° limit of the Apollo LRVs and Lunokhod-1, it is still unsuitable for the lunar south pole[6].

The circular wheel design on the current Martian rover has seen only a few modifications from the past lunar roving vehicles. It is known to sink into loose surfaces and lacks the traction needed to traverse steeper terrain[7]. This makes slippage increasingly likely as missions move towards more rugged lunar regions with loose regolith and icy patches.

Redesign means considering the off-world use of popular non-wheeled modalities seen on Earth. Carnegie Mellon's SnakeBot, for example, is a search and rescue robot that slides through debris with the help of its many mechanical joints[8]. If used on the Moon, this type of locomotion would enable the traversal of a wide variety of obstacles, albeit at a slow pace and without the capacity to carry the necessary instrumentation outlined in TX04 and TX08 of NASA's 2020 Taxonomy Report.

Boston Dynamics' BigDog, on the other hand, is a legged robot built for carrying equipment during military operations[9]. Capable of navigating 35° gradients and icy surfaces, this robot's locomotive system is a promising candidate for the lunar surface. Modifications to its weight and size are likely required to increase its slope limit and prevent tipping over during inclined travel.

Tank-like tracks introduce a form of locomotion that has already been proven successful in unfavorable terrains. Tracks have also been used in many military applications including the transportation of instrumentation and technology.

Morphing modalities involve transitioning from one method of locomotion to another without adding or removing parts. Most commonly, this transition is from wheel to leg. Currently, few wheel-leg hybrid robots exist beyond the research and development phase and those that do are limited in functionality and scope. One popular model proposed at the IEEE/RSJ International Conference on Intelligent Robots and Systems utilizes a traditional wheel where one half retracts into the other half to form a semi-circular leg (see Figure 3.1)[10]. These legs have the same axis of rotation as the entire wheel but at a more controlled rate of rotation thus enabling precise leg-like movements. This slight rotation, along with the translational motion provided by a sliding joint on the axle allows the legs to take measured steps across uncertain terrain. While this overarching concept is quite promising for traversing rugged surfaces, its "foot" curvature may encourage slippage on more inclined surfaces.

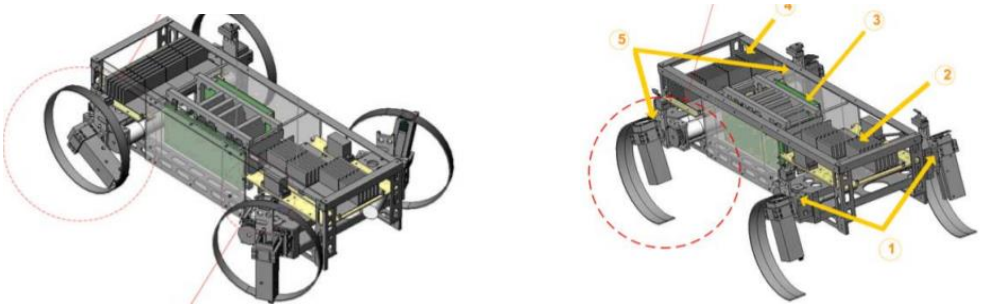

Figure 3.1. Computer aided design (CAD) drawings of robot operating in wheel (left) and leg (right) modes[10]

3.3 Overall Approach

Our morphing modality (Figures 2.1 through 2.3) design resolves issues that would likely be faced on the complex environment of the lunar south pole. Implementing four continuous track tank treads that can extend into legs enables reliable navigation of a variety of terrains. Unlike the leg design illustrated in Figure 3.1, our leg design mirrors the functionality of an actual leg through the incorporation of two joints that allow the modality to walk.

For flatter environments, such as those found in crater basins, the modality operates in "tank mode" with all four continuous tracks to traverse icy and jagged surfaces. For environments with more of a gradient, such as on the craters' walls, the morphing modality adopts "quadruped mode" (or "leg mode"). The treads function as feet with specialized gripping patterns, repeatedly being picked up and placed down with the help of the two joints. Given each appendage operates independently, the "tank" and "leg" modes can also be used simultaneously in "combination mode." For example, the front two can be in "leg mode" while the back two are in "tank mode," thereby enabling the safe traversal of unique lunar environments.

With these three modes of locomotion, this team is confident that this morphing modality solution will enable future rovers to overcome the locomotive challenges posed by the lunar south pole.

4.0 Project Description

The primary concept of combining tank driven motion with walking motion is achieved by wrapping a light-weight tank tread around the lower leg and designing quadruped actuators to accommodate the increased size and weight of the tread and motor.

There are many challenges to address when implementing such a design. For the quadruped, there are concerns about increased power usage for walking, the addition and distribution of weight onto the lower leg, and the difficulty in navigating complex terrain autonomously, which would require complex computer vision and control systems. Our solution integrates a lightweight motor towards the base of the lower leg joint to minimize the torque generated by the additional weight on the lower leg.

Treads have generally been excluded from space exploration. They have a short lifespan and are heavy,[(1)] two factors that individually disqualify any idea related to rover payloads. Our goal is to address both of those issues by removing common points of failure in tank treads such as the pins and joints and dramatically decreasing the weight of links[(2)]. For most earth-based systems such as construction vehicles, there has been little investigation into tank treads besides using rubber[(3)]. Polymer based tank treads are ill-fit for a lunar environment, and extreme environments in general since mechanical performance degrades dramatically[(3)]. Our tread design employs woven Kevlar to function as a connector between tread links, which we predict will result in a minor decrease in weight and much improved durability, strength, and performance in extreme heat and cold. Finally, we expect a significant decrease in weight by leveraging direct metal laser sintering (DMLS) or other technologies for 3D printing strong and lightweight tank links. 3D printing has the advantage of making the tank links bear a variety of loads since the percent infill can always be adjusted.

4.1 Phase 2 Development, Mitigation, and Changes

The focus of Phase 2 was the development of a quadruped platform for testing the tank to leg modality. As of this submission, the prototype development process remains ongoing. Sub-teams were formed to focus on five aspects of the design: tread, body design, leg design, software and electronics, and control and dynamics.

The overall concept of a morphing quadruped has remained the same from the proposal and Phase 1, but the method of implementation has changed. All design changes since the proposal have resulted from efforts to mitigate supply chain delays or due to eliminating unsuccessful prototypes. The most notable change is the case of the former, where all electronics and software from the Open Dynamic Robot Initiative (ODRI)

were no longer used in this design. The primary reasons for not using this previously proposed starting point platform were the global supply shortages and the cost and difficulty in manufacturing parts. Critical motor control chips were missing, cables and pin headers were no longer being manufactured, the custom motor pulleys were unjustifiably expensive, and modifications to the encoders were difficult to complete and prone to error.

Switching to a new implementation was a difficult decision and was made only after exhausting all possibilities. We contacted distributors, the ODRI research group contributors, attempted to purchase a pre-built system, and considered using other open-source projects. We tried using as many components as possible from ODRI, but this led to incompatibilities down the line. When one component is changed, the programming and physical design changes with it. These circumstances led to the decision to build a quadruped platform with off-the-shelf components. The selection of components is discussed in more detail in 4.3 Technical Specifications.

This decisive action reduced the amount of progress expected to be made at this stage of the project and this final stage of the challenge. We anticipated having a tested quadruped and morphing modality at the conclusion of the project given the ODRI design. Today, we are approaching the first prototype of the quadruped platform. However, even a rudimentary quadruped prototype can fulfill the purpose of evaluating the modality since the intent is to reflect its effectiveness.

Another significant departure from the original design was the decision to no longer use chainmail as the basis for connection between tank links. The infeasibility of iterating quickly given with a chainmail design became clear after the first few prototypes. The current tread design employs woven Kevlar as a space-grade replacement to classic pin and joint mechanisms used with tank treads. This woven Kevlar is sandwiched between two link components to increase traction with motion.

4.2 Overview of Current Progress

The following is an overview of the design, current state, and future work of the morphing modality prototype. It is divided between body design, tank tread, software and electronics, and motion planning.

Body design

- Internal layout and mounting mechanisms for components have been designed in CAD.
- Future work:
    - Manufacture, assemble, and integrate the electrical components into the main body
    - Investigate heat dissipation and flow through the interior during usage
    - Develop designs that mitigate dust after initial testing

Leg Design

- The ODRI leg was modified to accommodate an off the shelf encoder and additional wire management.
- The expensive motor gear system was re-designed to reduce the cost.
- The team assembled and built a functioning, full-leg prototype that is controllable via external interfaces.
- Future work:
    - Assemble a complete set of legs and attach it to the body
    - Reduce exposed parts and take design dust mitigation measures for testing in environments with finer particles

Tank tread

- Several iterations of tread design were prototyped, and unviable designs have been eliminated.
- Design has been switched from a chainmail design to a Kevlar based one
- Future work:
    - Weave remaining connectors and mount tank links to sprocket system

- Improvement of weaving process - look for outsourcing opportunities
- Finalization of tread links are still required. Plans to use alternative manufacturing methods to significantly reduce the link weight as well as investigate the durability of such a design

Software and Electronics

- The electronics parts list was finalized, and communication, power, and control have been verified for components individually.
- Small scale tests of six motors verified scalability of motor control interface and should scale to eight or more motors.
- Future work
    - Integration with the body after the manufacturing of the internal body components
    - Developing supervisory control for tread and walking motion
    - Integration of control code with ROS to use existing packages,
    - Enabling medium range communication/control (~50 ft range)

Motion Planning

- Inverse Kinematics analysis of legs was performed.
- Trajectory generation using high order polynomials was performed.
- Statically stable gait designs have been iterated.
- Future work:
    - Inverse Dynamics analysis of legs
    - Dynamically stable gait designs
    - IMU feedback control
    - Foothold Placement Planning using LiDAR
    - Advanced control and optimization paradigms such as MPC (model predictive control), feedback linearization, iLQG (iterative linear-quadratic-Gaussian control), deep reinforcement learning. See 4.2 for Prototype Components

4.3 Prototype Design

4.3.1 Full Body

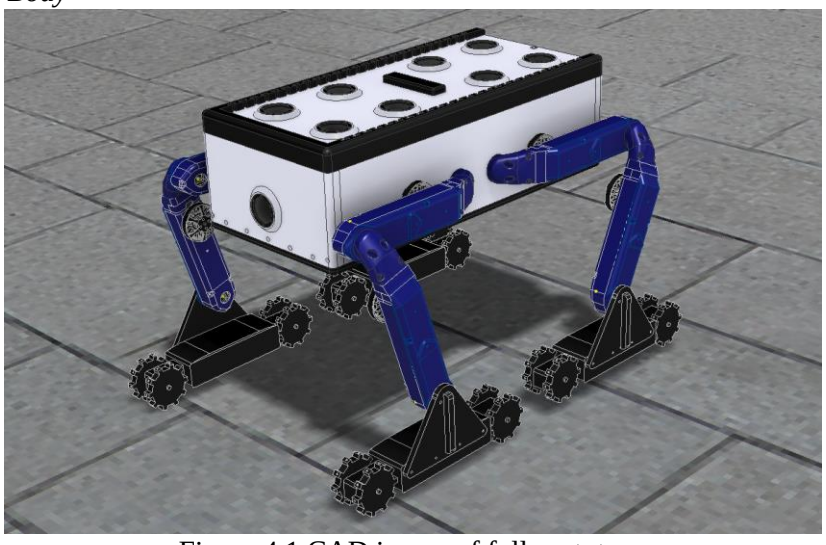

Figure 4.1 CAD image of full prototype

The body, as seen in Figure 4.3 and Figure 4.3, contains parts that are integral to the performance of the rover.

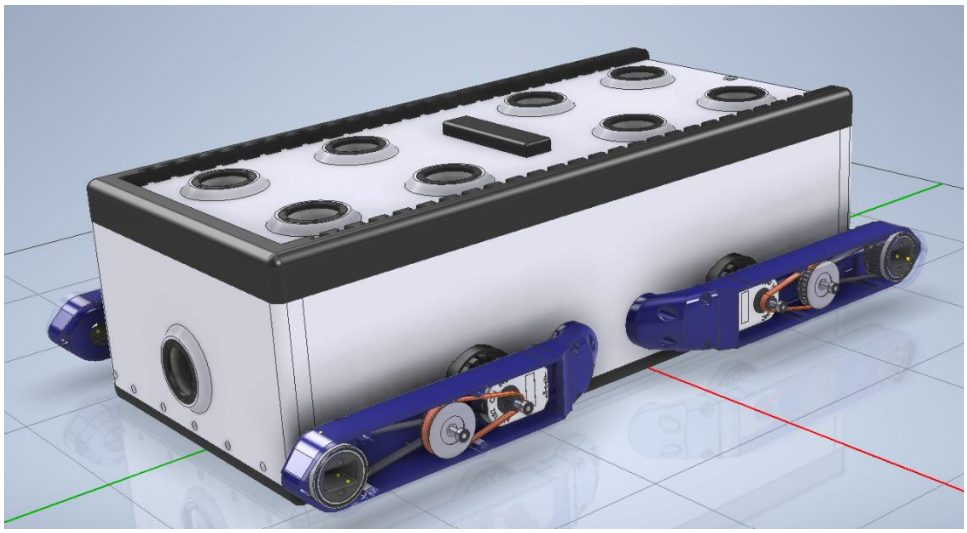

Figure 4.2 CAD image of outer body design

Six ODrives, responsible for the control of the 8 leg motors, are placed near the center of the body, minimizing their distance from the legs they direct. The angular and translational position of the body is monitored by the IMU sensor, and power is supplied through 2 batteries located on either side of the body. These components, as well as the Raspberry Pi (from which the controls and sensors of the rover were programmed) are suspended by a network of mesh dividers and trays. These pieces contain holes in a mesh pattern to allow for wires to easily pass through them and fit securely into the grooves that line the side walls. The height of the dividers matches that of the lid, which restricts movement for the internal components even if the rover is flipped over. These are screwed onto dividers.

The side walls and lid contain holes with air filters that function with a fan on the back to facilitate proper ventilation avoiding dust contamination. When unsecured, the lid of the body slides out, allowing for easy assembly and maintenance.

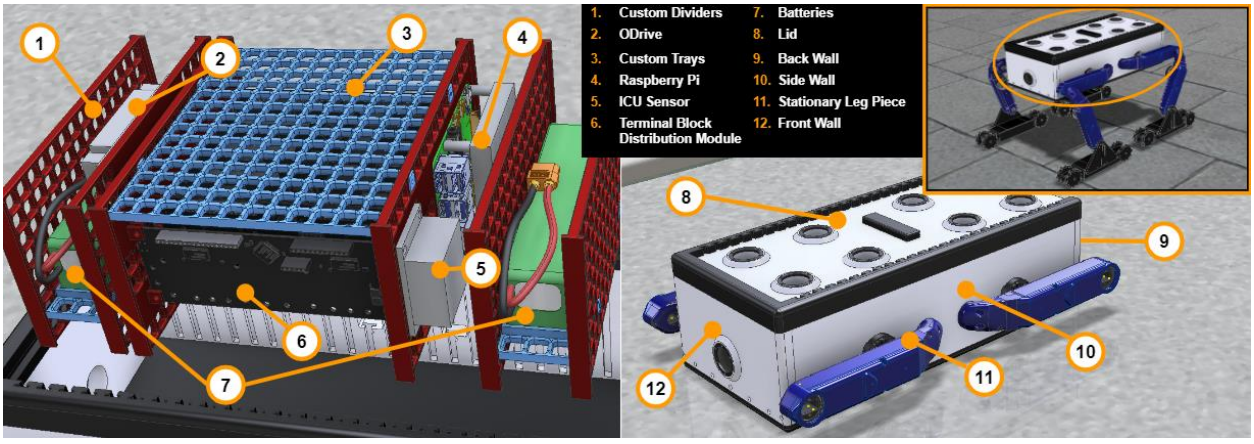

Figure 4.3 CAD image of inner body design

4.3.2 Leg

Upper Leg:

The innovation of our modality idea comes from the versatility of its legs. When walking, the motors within the upper leg sections, seen in Figure 4.4, work to control the angular position of the parts that succeed them. This keeps the "feet" moving along a smooth walking path.

When driving, these parts remain stationary. The first section of the lower leg angles itself towards the ground, providing the tread with maximum terrain contact. When traversing hills, the upper leg section can assist the rover's driving mode, reposition to maximize tread contact, lower the rover's center of gravity, and improve the overall handling. The joint between the upper and lower leg sections creates an additional suspension component, acting as a passive independent strut, compressing, to absorb stress for each set of legs/tracks. This further improves the handling of the modality when in its driving mode.

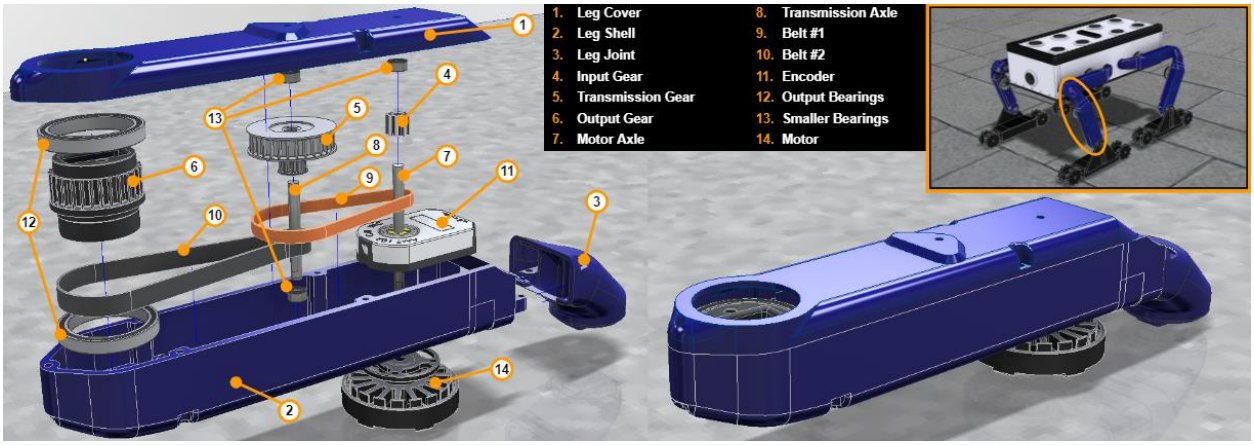

Figure 4.4 CAD breakdown of components in upper leg

Numbers in [] in this section reference Figure 4.4. Rotational power is provided through the Antigravity MN4004 KV300 motor [14]**[(1)],** with an AMT102-V**[(2)],** encoder [11] attached to keep track of the leg's angular position. To improve torque, the angular velocity is reduced via a transmission of belts [9,10] and a concentric double-gear [5], before connecting to the output gear [6]. This is where the next leg section attaches.

The leg casing is comprised of 3 removable 3D printed parts to facilitate effective maintenance and assembly. Screws line the borders of the cover and shell, with 2 more fixing the joint to the shell upon assembly. The shell and cover contain notches and ridges to keep bearings, axles, and wires in place. In the upper leg, wires are fed through the output gear [6] and then lifted above the internal components in the shell [2], as seen in Figure 4.5. The wires are supported by hooks placed across the cover [1], as seen in Figure 4.6, before being fed through the leg joint [3] and into the next leg part.

Figure 4.5 3D printed upper leg shell [2]

Figure 4.6 3D printed upper leg shell cover [1]

Lower Leg:
Numbers in [] in this section reference Figure 4.7. The lower leg, as seen in Figure 4.7, is an attachment between the upper leg and tread. Using a triangular connection piece [1], the tread is given more movement

in the form of active suspension and does not require spring suspension within the tread itself. The lower leg houses a ROB-15277 brushless motor, located in the body [4], which provides power to one set of gears [3]. Those gears are then attached to the other set of gears using the tread. The second set of gears are adjustable in length to allow tension of the tread [6]. The wires are fed through the back of the triangle connector piece and further fed through the upper leg into the body [8].

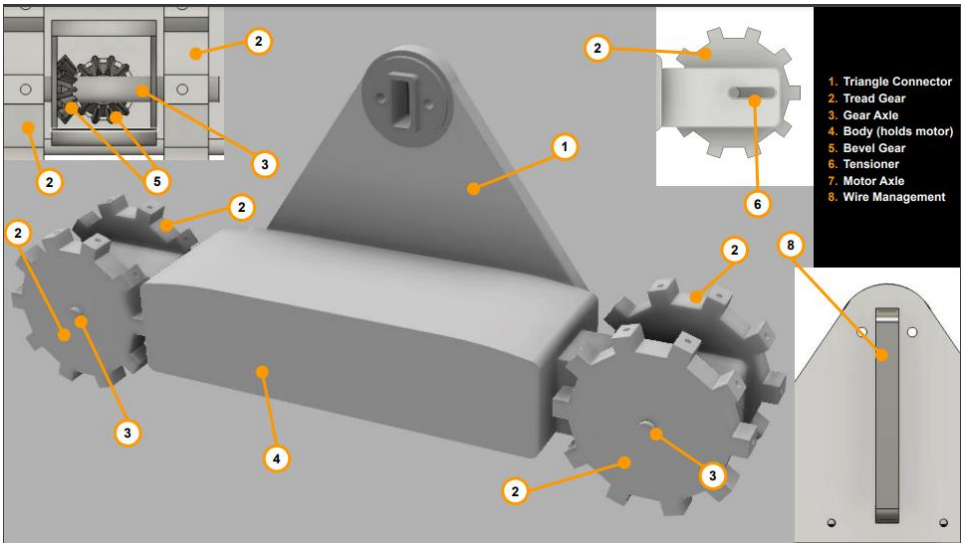

Figure 4.7 CAD components of the lower leg

4.3.3 Tread

Instead of using chainmail to achieve flexibility without mechanical joints, as previously mentioned, Kevlar was weaved, as seen in Figure 4.8, into two strips to accomplish this desired attribute. The Kevlar is weaved in a plain weave pattern by laying 23 strands lengthwise on a loom and then using a needle to weave strands perpendicular to the lengthwise strands to in an over-under pattern.

Figure 4.8 Plain weave Kevlar strip

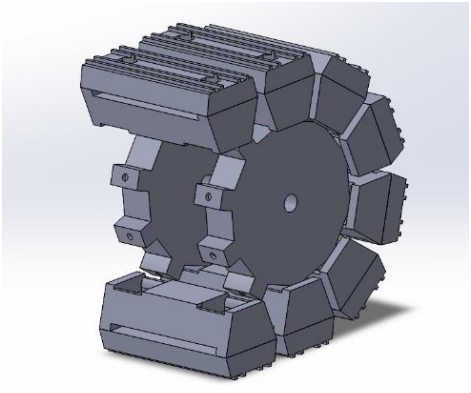

Figure 4.9 Sprocket and tread link interface

The ends of the weave were attached with a specialized tread link allowing the ends to overlap, also providing minor length adjustments. The Kevlar provides both tensile strength, flexibility, resilience to cosmic radiation and large temperature changes [(4)] 3D printed tracks are attached to two Kevlar loops via clamping design with two bolts that penetrate the Kevlar weave, as seen in Figure 4.9. The distances between the tread links are tightly controlled using a custom designed spacing jig, which places each link

the same distance from the center of the pervious link. 3D printed versions of the links and gears are shown in Figure 4.10 and Figure 4.11.

Figure 4.10 3D printed upper and lower links for tread

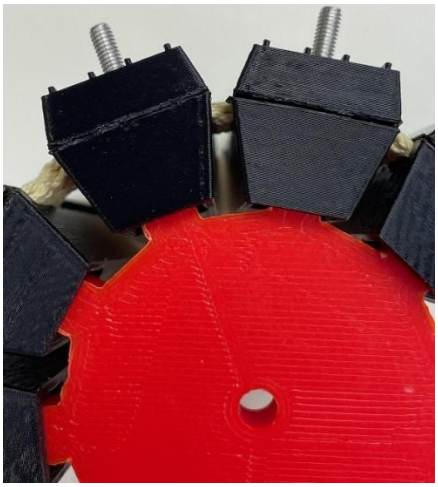

Figure 4.11 Links going around 3D printed gear

4.4 Code Overview

The following two references refer to the code this team has uploaded to public sites that can be modified and used, and links to this team's code is provided in Appendix A: Organization page[(1)] and Main Codebase.[(3)] The organizations page includes various repositories used as dependencies as well as the main codebase, amberrobot. Within amberrobot, there are files for controller software, which binds keys on a controller to specific motor functionality (rust-client/src/controller); IMU software, which is used for hardware communication to an IMU (rust-client/imu); odrive software, which is used for hardware communication to the odrive (rust-client/rustodrive); dynamics and kinematics software which was used to generate a trajectory which is then used for the legs to follow (rust-client/kinematics).

The flow of the operating system connecting these programs to AMBER's hardware is illustrated in Graph 4.1.

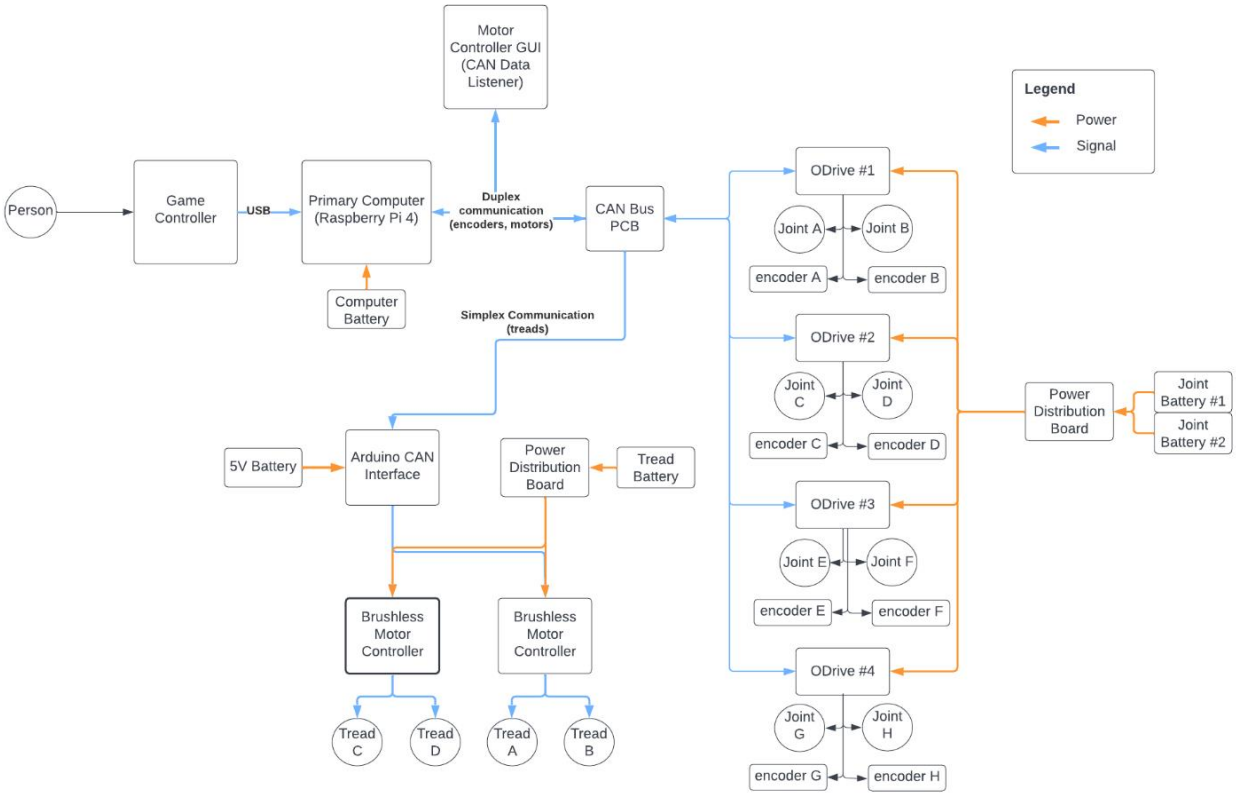

Graph 4.1 Component power and communication diagram.

4.5 Motion Planning: Kinematic Analysis

5.2.1 Inverse Kinematics

This quadruped robot consists of a rigid body and four legs with two degrees of freedom (each leg has the same structure). The links of the legs are connected to each other by rotary joints.

Depending on the coordinates of the legs, the robot body can have different configurations. For this reason, the kinematic equation between the rotational movements around the center of the body's coordinate system and the coordinate system of each endpoint of the leg (end-effector) is investigated. Initially, to determine the position and orientation of the robot center of the body in the workspace, the transformation matrix is obtained using the homogenous rotation matrices (following the Denavit-Hartenberg Convention) for the hip joint and for the knee joint given in equations (1) and (2):

$$H_1^0 = \begin{bmatrix} c_1 & 0 & s_1 & a_1 \times c_1 \\ s_1 & 0 & -c_1 & a_1 \times s1 \\ 0 & 1 & 0 & 0 \\ 0 & 0 & 0 & 1 \end{bmatrix} \quad (1)$$

$$H_2^1 = \begin{bmatrix} c_2 & -s_2 & 0 & a_2 \times c_2 \\ s_2 & c_2 & 0 & a_2 \times s_2 \\ 0 & 0 & 1 & 0 \\ 0 & 0 & 0 & 1 \end{bmatrix} \quad (2)$$

The above matrices are multiplied to determine the total transformation matrix, which will represent the complete system. The total transformation matrix T is given in equation (3) where: $T = H_2^0 = H_1^0 \cdot H_2^1$

$$T = \begin{bmatrix} c_1 \times c_2 & -c_1 \times s_2 & s_1 & c_1\,(a_1 + a_2 \times c_2) \\ s_1 \times c_2 & -s_1 \times s_2 & -c_1 & s_1\,(a_1 + a_2 \times c_2) \\ s_2 & c2 & 0 & a_2 s_2 \\ 0 & 0 & 0 & 1 \end{bmatrix} \tag{3}$$

In the following equations, *x*, *y*, and *z* are the final coordinates of the corresponding axes of the endpoint for the quadruped's leg. The first three values of the fourth column of the transformation matrix *T* represents the values of *x*, *y*, and *z*, respectively.

$$x = (a_1 + a_2 * \cos(t_2)) * \cos(t_1) \tag{4}$$

$$y = (a_1 + a_2 * \cos(t_2)) * \sin(t_1) \tag{5}$$

$$z = a_2 * \sin(t_2) \tag{6}$$

The Inverse Kinematics Solutions are given in equations (7) and (8):

$$t_1 = atan2(y, x) \tag{7}$$

$$t_2 = atan2\left(z, \left(\sqrt{(x^2 + y^2)} - a_1\right)\right) \tag{8}$$

where, $t_1$and t_2 are the angles of the hip-joint and knee joint.

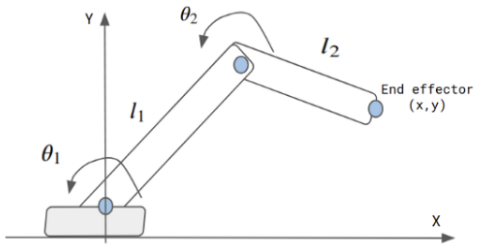

$$\begin{bmatrix} x \\ y \end{bmatrix} = \begin{bmatrix} l_1 \cos\theta_1 + l_2 \cos(\theta_1 + \theta_2) \\ l_1 \sin\theta_1 + l_2 \sin(\theta_1 + \theta_2) \end{bmatrix}$$

$$\begin{bmatrix} \dot{x} \\ \dot{y} \end{bmatrix} = J \begin{bmatrix} \dot{\theta}_1 \\ \dot{\theta}_2 \end{bmatrix}$$

5.2.2 Jacobian Matrix

The Jacobian matrix is used to linearize the inverse kinematics of the leg and to achieve velocity commands in the direction of the kinematic solution. It provides the relation between joint velocities and end-effector (endpoint of the leg) velocities of a leg.

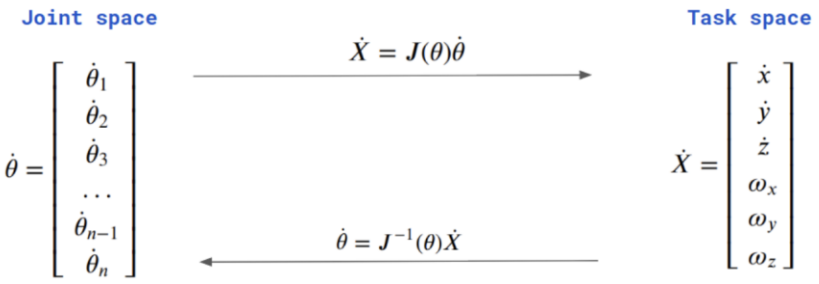

4.6 Motion Planning: Path Planning

4.6.1 Trajectory Generation at the Joint Level

The trajectory planning for the leg follows the following hierarchy:

1. Task planning – Designing a goal, such as taking a step towards a particular direction.
2. Path planning – Generating a feasible path from a start point to a goal point. A path usually consists of a set of connected waypoints or control points.
3. Trajectory planning – Generating a time schedule for how to follow a path given constraints such as position, velocity, and acceleration.
4. Trajectory following: Once the entire trajectory is planned, gaits execute it accurately.

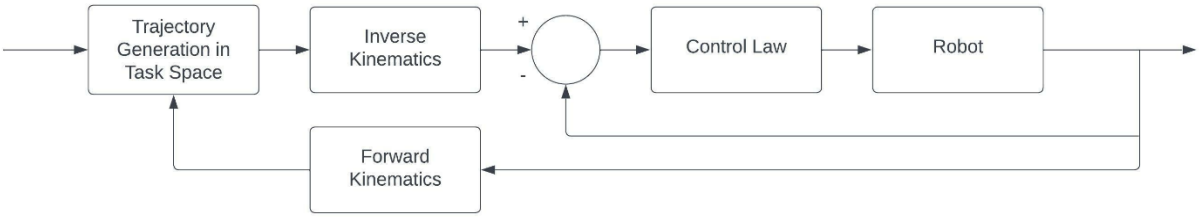

Block Diagram for Task Space Trajectory Generation

For the leg to take a step, the end of the leg (end-effector) must follow a certain trajectory. Hence, task-space trajectory planning is performed, and thus inverse kinematics must be solved at every time step. Polynomial trajectories are useful for continuously stitching together segments with zero or nonzero velocity and acceleration because the velocity and acceleration profiles are smooth. Hence, we use higher-order polynomials like Bézier and b-spline curves to generate trajectories for the end of the leg.

During the swing phase (foot first leaves the ground and ends when the same foot touches the ground again), higher order Bézier curves can be used as trajectories. The two concerns are:

1. Generating control points
2. Impact with the ground on contact

We use De Casteljau's algorithm, a recursive method to evaluate polynomials in Bernstein form or Bézier curves, to generate higher-order Bézier curves. We feed this algorithm pre-selected control points based on step length and height, and swing, flight, and stance phase durations. This algorithm generates a parametric polynomial equation in t, $0 \leq t \leq 1$.[(4)(5)]

We programmed another trajectory that tracks the leg of a cheetah, a compound cycloid, from the research paper "Single-Leg Structural Design and Foot Trajectory Planning for a Novel Bioinspired Quadruped Robot." It has an advantage that it can reduce the inertia causing velocity and acceleration to be zero at touchdown, which is at the end of the flight phase when the leg touches the ground resulting in zero impulse. The equation of the trajectory is as follows:

$$x = S\left[\frac{t}{T_m} - \frac{1}{2\pi}\sin\left(2\pi\frac{t}{T_m}\right)\right] - \frac{S}{2},$$

$$y = \begin{cases} 2H\left[\frac{t}{T_m} - \frac{1}{4\pi}\sin\left(4\pi\frac{t}{T_m}\right)\right], & 0 \le t < \frac{T_m}{2}, \\ 2H\left[1 - \frac{t}{T_m} + \frac{1}{4\pi}\sin\left(4\pi\frac{t}{T_m}\right)\right], & \left\{\frac{T_m}{2} \le t < T_m, \right. \end{cases}$$

where S is the stride length, H is the step height of the flight phase and T_m is the period of the flight phase.[6]

4.6.2 Gaits

There are two broad categories of quadruped robot gaits: Statically Stable and Dynamically Stable. We implement a popular statically stable gait called creeping gait in which one leg is lifted at a time and there are three stance legs at any moment. The duty factor (the percent of the total cycle which a given foot is on the ground) for this gait is ¾. This is not efficient in comparison to galloping gaits that have a duty cycle of ½ but has the advantage of not tipping over[7].

A statically stable gait will not fall even when all its joints freeze, whereas a dynamically stable robot requires constant motion to prevent it from falling. If the center of gravity projection on the ground is inside the support polygon framed by the leg tips the gait is statically stable. This is the main criterion we strove to maintain.

One gait cycle is divided into eight different periods, as seen in Figure 4.12. Four legs of the quadruped repeat the motion individually in a certain order from the stance phase to the swing phase to achieve walking using creeping gaits. The gait sequence is (leg4→leg2→leg3→leg1). The swing phase is implemented using trajectories in the previous subsection.

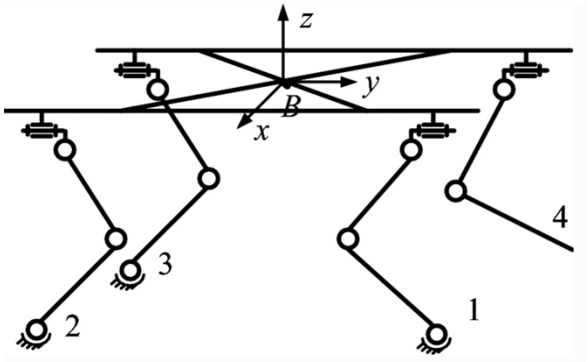

Figure 4.12 Creeping Gait Sequence[7]

4.6.3 Control Law

ODrive, the off the shelf motor controller used, is a cascaded position style position, velocity, and current control loop. There are several control modes such as position, velocity, ramped velocity, torque, etc., that use various stages of the control loop. Each stage of the control loop is a variation on a PID controller. We use a combination of position and trajectory control modes, the latter to aggressively tune the feedback gains ensuring smoother motion. The position feedback in this control loop comes from the incremental encoders used[9].

After computing inverse kinematics equations and adjusting for the gear ratio, the resulting joint rotations are communicated to the ODrive to turn the motor.

4.7 Technical Specifications

The codebase consists of Rust for hardware communication and trajectory generation and Python for testing and debugging the motor controllers. Rust was effective at speeding up development but did not have direct interoperability with C++, a widely used programming language, libraries. For the purposes of motor control, this was allowable since the codebase was standalone and required few extra dependencies. In the future we will finish the integration with the Robot Operating System (ROS) to take advantage of the plethora of already existing quadruped control libraries, while enjoying the advantages of Rust.

The Raspberry Pi 4 was the target of our builds and was the supervisory controller for the motor controllers.

The ODrive motor controller [(5)] was selected due to excellent documentation, availability, and compatibility with a variety of brushless DC motors (BLDC) and encoders. The guidance given by the ODrive community forum was invaluable and saved countless hours of work in configuration and development. The ODrive platform is language agnostic since it supports communication via Controller Area Network (CAN) and allows for the chaining of motor controllers in a bus design. CAN was preferred since it allowed for duplex communication, speeds of up to 1 Mb/s, and communication to a large number of motor controllers. The protocol was pre-defined by the ODrive project and was implemented in Rust. Additionally, we developed a user interface for visualizing the statuses of the motor controllers. We open-sourced our beta client library for the ODrive community to use for future projects.

To prevent ground loops or back-emf from damaging the single board computer, we purchased an isolated CAN board. The computer and motors are powered by separate batteries to completely decouple the power of the motors from the power of the computer. We designed a simple printed circuit board (PCB) for the motor controllers and computer to communicate with one another.

The encoders used were CUI AMT102-V and are a deviation from ODRI's selection. A significant amount of time was spent integrating the ODRI's encoders with the motor controllers. There was signal, noise, and power issues, which proved to be more of a problem than it was solving one. We purchased the encoders recommended by the ODrive community, and they worked well immediately.

The motors selected were the Antigravity MN4004 KV300 brushless DC motors. These motors allow for fast acceleration and have a longer lifespan than brushed DC motors[(6)]. These are the same motors used in the ODRI design. Brushless motors have a higher starting velocity and low starting torque. The actuator design has a gear transmission to output the required torque and velocity characteristics.

Selection of the tread motors required particular care since weight and torque outputs are extremely important to the performance of the tread and the leg. If the motor weighs too much, we hinder the agility of the actuators. If the motor is not powerful enough, the rover in tread mode may not be able to propel itself forward. We selected two candidate motors for testing, one that functions at 140 RPM and the other at 200 RPM, both of which are brushed motors. Brushed motors were preferable since the form factor fits best with the lower leg actuator and high-performance was not as necessary for the treads as it is with the joint motors. These two motors had the highest available stall torque per unit weight. A set of each motor was purchased to test both options. The 140 RPM motor had stall torque [Nm/kg] of 1.496 while the 200 RPM motor weighed twice as much and had a stall torque per kilogram [Nm/kg] of 0.586. While stall torque is not directly indicative of rated torque (torque at a specific rotational velocity), the manufacturers did not detail the torque speed curve. The motors have similar dimensions and are interchangeable if more torque, or if more speed is desired.

The tank tread motors are brushed motors, are not compatible with the ODrive motor controllers, and require a different motor control scheme. Since tank tread motion does not require complex and precise control, we were able to buy inexpensive and readily available brushed motor controllers. The simplicity of the tread motor controls resulted in needing to develop an interface for communication from the Raspberry Pi to the brushed motor controller. An extension to the CAN communication codebase is being developed to communicate with an Arduino, which is tasked with receiving and executing CAN commands for the brushless motor controllers.

We implemented the drivers for a more cost-effective inertia measurement unit (IMU) than the one used in the ODRI for future use in a more advanced prototype.

For end user robot control, we are using a game console controller as user input. The received state of the controller will be processed and converted into appropriate joint commands. Currently the remote communicates via USB, but Bluetooth is supported. In the future we will investigate using radio frequency transmission for testing at longer ranges.[7]

The body, leg shells, tread links, and various gears were 3D printed using polylactic acid (PLA). This method allows to vary the density of the components as needed.

The ODrive v3.6 24V version has a peak current of 120A per motor. This can power the Antigravity MN4004 KV300 motors, which have a 4-6S lipo range, 9A maximum current, and 216W maximum power. Since motor controllers ('ESC' - Electronic Speed Control) take a high voltage and low current power source and, though pulse width modulation (PWM)[12], converts it into a low voltage and high current for use with a motor, we use batteries with low current but high discharge rates. LiPo (Lithium Polymer) batteries are suitable due to their lightweight, high discharge rates, and good capacity.

The motor has a maximum RPM (revolutions per minute) of 5000, maximum current of 5.2A at maximum RPM and KV (constant velocity) of 300.

The maximum required voltage can be calculated using the following equation:

$$V_{PSU=}\frac{RPM_{max}}{KV}\times 1.25 \approx \frac{5000}{300}\times 1.25 \approx 20.83V$$

where, V_{PSU} is the power source voltage.
The maximum required power can be calculated using the following equation:

$$P_{max} = I_{max}\times V_{PSU}\times 1.25 \approx 5.2\times 20.83\times 1.25 \approx\ 135.395W$$

where P_{max} is the maximum power consumed.

As a result, the load (current) is 135.4W/20.83V = 6.5A. Therefore, a battery life of 45-60 minutes at maximum power consumption the battery capacity is around 5300mAh (milli amp hours). Based on the above calculations, we select two 3S Lipo batteries with capacity 5200mAh, 80C (discharge rate) and 57.72Wh (energy) connected in series to achieve a total voltage of 6S, where 1S is the voltage of one cell, i.e., 3.7V. This setup provides power to four ODrives connected in parallel using a power distribution board to maintain the potential difference. To increase safety, XT-60 connectors (anti-spark connectors) are used at all power terminals.

The tread motors (brushed DC) have a separate low power system to avoid a single point of failure. They are powered using 9V alkaline batteries [13].

4.8 Assumptions

When creating the design for a lunar rover with a morphing modality, the team made several assumptions when it came to the performance and practicality of the design. One such assumption was that the difference in gravitational pull on Earth and on the moon would not affect the performance of the modality. Another assumption made was that the modality's performance in extremely cold temperatures could be emulated and evaluated using cryogenic conditions on Earth. In terms of the practical use of the rover and its modality, one assumption the team made was that the design would be easily transferred to NASA for further research and development. This means NASA would be able to pick up from where the team left off and efficiently improve upon and finalize aspects of the design without gaps or unnecessary delays. It was also assumed that minimal maintenance would be required and once on the moon, there would be no need for physical support. Lastly, for practicality during launch, it was assumed that the modality design is compactable and durable enough for launch.

4.9 Funders and Stakeholders

Potential robotics stakeholders that can benefit from the design include Apptronik, HoneyBee Robotics, Boston Dynamics, and Maxar Technology. Apptronik is a partner with NASA's National Aeronautics and Space Administration that focuses on developing humanoid robots. Apptronik can benefit from AMBER's mobility and leg design to push the next generation of general-purpose robots. HoneyBee Robotics, recently acquired by Blue Origin, creates next-generation applications in important commercial and exploration flight missions. The company has worked previously with NASA and other space exploration companies. They could benefit from our project as they have expertise in motion control systems, exploration systems, and infrastructure systems research divisions. Boston Dynamics is a renowned robotics manufacturer known most for their design of "The Agile Mobile Robot." The use of appendages in the design of the modality and their expertise in creating robots that use that particular mode of transportation could prove valuable. Maxar Technology is another robotics manufacturer with a focus on space designs. They have worked on both commercial and government programs, including working directly with NASA to create robotic arms that were included on the Mars Rover.

5.0 Verification Testing on Earth

As previously mentioned, the decision to move away from using the ODRI as a platform to build off resulted in the team starting the design of this modality from a lower technology readiness level. This decision, though necessary, resulted in less time for verification testing of the modality. A great deal of time has been spent ensuring the software to hardware connectivity is strong so that when further prototype testing becomes possible, the tests will be evaluated with a strong foundation in the functionality of the software and hardware itself.

5.1 Simulation

MuJoCo simulation to verify kinematic and preliminary dynamic modelling of an 8dof quadruped using the MuJoCo Menagerie "unitree_a1" model. This model contains a simplified robot description (MJCF) of the A1 Quadruped Robot developed by Unitree Robotics. It is derived from the publicly available URDF description.

MuJoCo (Multi-Joint Dynamics with Contact) is a free and open-source physics engine. It is a simulator for high speed, accuracy, and modeling power mainly designed for computationally intensive control techniques[9]. By using this simulation, even with a quadruped other than our own, we were able to verify our equations used in Sections 4.5 and 4.6 worked. In the future, our prototype will be compiled into this simulation to do further computational testing.

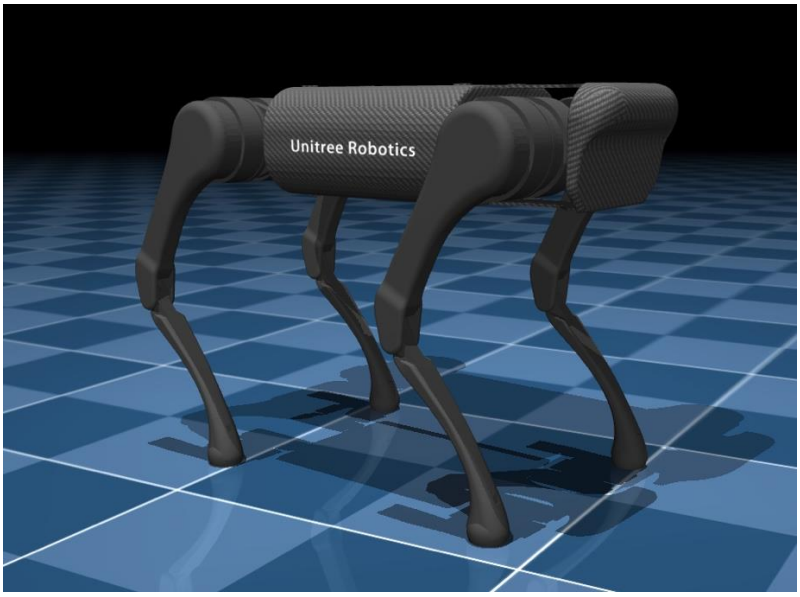

Figure 5.1 Still-frame from MuJoCo software

5.2 Testing Not Performed

The team built a miniature articulating base slope lab, to qualitatively test the mobility of the rover on ambient sand at different degree slopes. team established a connection with the slope lab at Glenn Research Center for future testing. We were unable to make the trip due to time constraints and the progress made on the rover at the time travel would have been optimal. However, it was reported to the team that we are welcome back for testing in the future.

The team had planned to evaluate the rover on an ice rink to test how it would move on icy surfaces. Contact was made with the Bolton Ice Palace in Bolton, CT, and approval for testing was given. This testing was not performed due to concerns about the cold environment potentially damaging the electrical components and time constraints.

The team also planned Drawbar Pull (DP) tests in a variety of environments. These tests would determine the gross pulling force of a vehicle thus conveying the tractive effort of that vehicle. The plan was to perform this test in ambient conditions in LHS-1 lunar simulant soil and frozen simulant soil. Other environments to perform a DP test are in a high vacuum environment, simulating the pressure that exists on the moon; and a cryogenic environment, simulating the low temperatures on the lunar surface.

6.0 Safety Plan and Protocols Followed

In the construction and test of the AMBER prototype, safety concerts were top priority. Procedures are categorized by hazard type: physical, electrical, chemical, and particulate. The hazard types are defined as follows. Each category involves certain general measures for risk mitigation that guide safety procedures. Table 6.1 shows tools and items used which have an elevated risk of posing hazards. Always read the Material Safety Data Sheet (MSDS) for any materials which will be used and utilize proper Personal Protective Equipment (PPE) for the task.

Physical: Harm may be caused due to the physical property of an object, for example sharpness, weight, or heat.

- **Heat:** Treat all heating elements as if they are hot, even if they are not. Do not directly touch hot surfaces until you can hold the back of your hand 3 or 4cm away without feeling heat.

- **Sharp objects:** When carrying sharp objects, i.e. knives, ensure the sharp portion is pointed down. When giving someone a sharp object, do not hand them the sharp portion. When using a sharp object, make sure that no one is within an arm length radius.
- **Power tools:** When using tools with motorized elements

Electrical: Hazards due to the electrical properties of a device or stored electrical energy, for example, a power supply or charged capacitor.

- Ensure all electronics are unplugged and capacitors are safely discharged before handling power electronics.

Chemical: Harm that may be caused due to the chemical properties of a substance by contact, inhalation, or ingestion. Always consult the Material Safety Data Sheet (MSDS) before using a chemical item. The MSDS will always be made easily accessible and pertinent information (i.e. necessary PPE) will be clearly labeled on the container.

- Consult the MSDS before starting work to determine the proper handling procedure and PPE.
- Do not eat or drink in the work area to avoid contamination.

Particulate: Harm caused by coarse or fine granular material. Special mention is made of this category to highlight safety procedures for handling lunar regolith simulants.

Item	Hazard categories	Notes and specific measures
Soldering iron	Physical, Chemical	**Physical:** Soldering irons get hot. Even if the iron is off, only handle the iron by the grip, not the metal portion. The iron may retain enough heat to cause harm minutes after being unplugged. Use safety glasses when soldering as molten solder may easily flick back at your face when cleaning the iron. **Chemical:** Consult the MSDS for all soldering materials, I.e. flux, solder, and tinning compound. Avoid touching flux directly. Only solder in a well-ventilated area.
Knives and blades	Physical	
Hand saws	Physical	
Drill and rotary tool	Physical	**Physical:** Ensure you are wearing safety glasses and are not wearing any loose garments or jewelry. If necessary, tie hair back to avoid entanglement. Holding a part with the other hand is not sufficient work holding, always use clamps to hold down your workpiece. After an operation is complete
PCB Printer	Physical, Chemical	**Physical:** Avoid drill when moving. Avoid touching when bed is heated **Chemical:** Perform in a fume hood to avoid toxic fumes from conductive and solder paste

Table 6.1 Commonly used tools, hazard categories, and specific measures for risk mitigation.

7.0 Path-To-Flight

The modifications needed for the design to be used on the moon include dust mitigation measures, mechanical and electrical components to regulate temperature, and low vacuum-grade motors. To address dust mitigation, the components must be sealed and as few exposed parts as possible. The ability for the mechanical and electrical components to sustain drastic temperature changes must be addressed by developing systems to regulate component temperatures, especially given the insulation and sealing necessary for dust mitigation. The high vacuum (10^{-3} psi) is an additional qualification that must be met to ensure the modality is ready for flight.

Prior to building flight hardware, the essential design framework includes constructing a ruggedized leg. The leg design included changes to the y-bar design and the change in construction from 3D printed parts

to machined parts. A new test stand (sandbox with tread and motor) is needed to test parameters including traction, slippage, and suspension (in progress via Becker–Döring cluster equations) for the Prototype 2 Kevlar. The current design includes a thicker and larger tread to increase durability.

More precise research on Martian conditions needs to be explored. After assessing the concept on the regolith at Glenn Research Center-Rocky Slope Lab, a better determination can be made if there is the capability to traverse Martian terrain.

The conclusion of this challenge is not the conclusion of this project. AMBER has a permanent home at the University of Connecticut. The project will transition into a student organization where undergraduates for years to come will use this project as a learning platform and to progress its sophistication. Excess funding will be used to continue development and testing, and additional funding sources, such as writing grant proposals to the VT Space Grant Consortium, will be pursued. It is the desire of the team to keep the project primarily in the hands of undergraduate students, as opposed to leaning heavily on faculty. This follows the foundation with which this team was formed on, and its students are confident in the technology's ability to influence individual lives as well as progress to the point of reaching the Moon.

8.0 Results and Conclusions

More time is needed for development and testing of all four appendages, followed by testing in simulated environments. Quadrupeds are complicated systems, and the setback of being unable to use the ODRI as intended puts the team in the position of developing the quadruped platform before any testing can begin. It cannot be determined at this moment if morphing modality will operate and perform as expected, but the continuation of this project post-challenge is actively being investigated.

9.0 Timeline

9.1 Phase 1

Task	Start	End
Phase 1: February 22 - May 25		
Purchasing material	2/21/22	5/17/22
Investigated procurment of ODRI components	2/24/22	3/29/22
Designed MSL	3/7/22	3/23/22
Learning programming language: Rust	2/29/22	4/26/22
3D printed ODRI components	3/8/22	4/13/22
Recruited 10 new members	3/15/22	3/21/22
Developed testing procedure for MSL	3/20/22	4/7/22
Designed and assembled first iteration of chainmail treads	3/26/22	4/5/22
Demonstrated software stack functionality: Rust, Docker, ROS	3/28/22	4/17/22
Decided to move away from ODRI	4/12/22	4/19/22
Selected off-the-shelf electrical components	4/11/22	5/18/22
Designed inner gear transmission for lower leg	4/23/22	4/30/22
Reevaluated chainmail treads and pursued kevlar weaving instead	4/25/22	5/3/22
ASCE Earth and Space Conference	4/21/22	4/27/22
Developed systems engineering methedologies	4/30/22	5/25/22
Began redesigning shell structure	5/1/22	5/23/22
Mid-project report	5/10/22	5/24/22

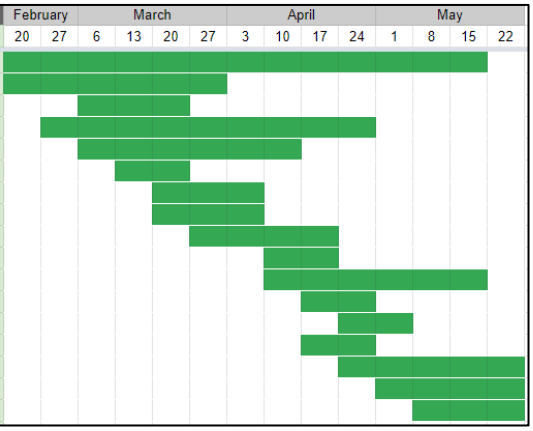

9.2 Phase 2

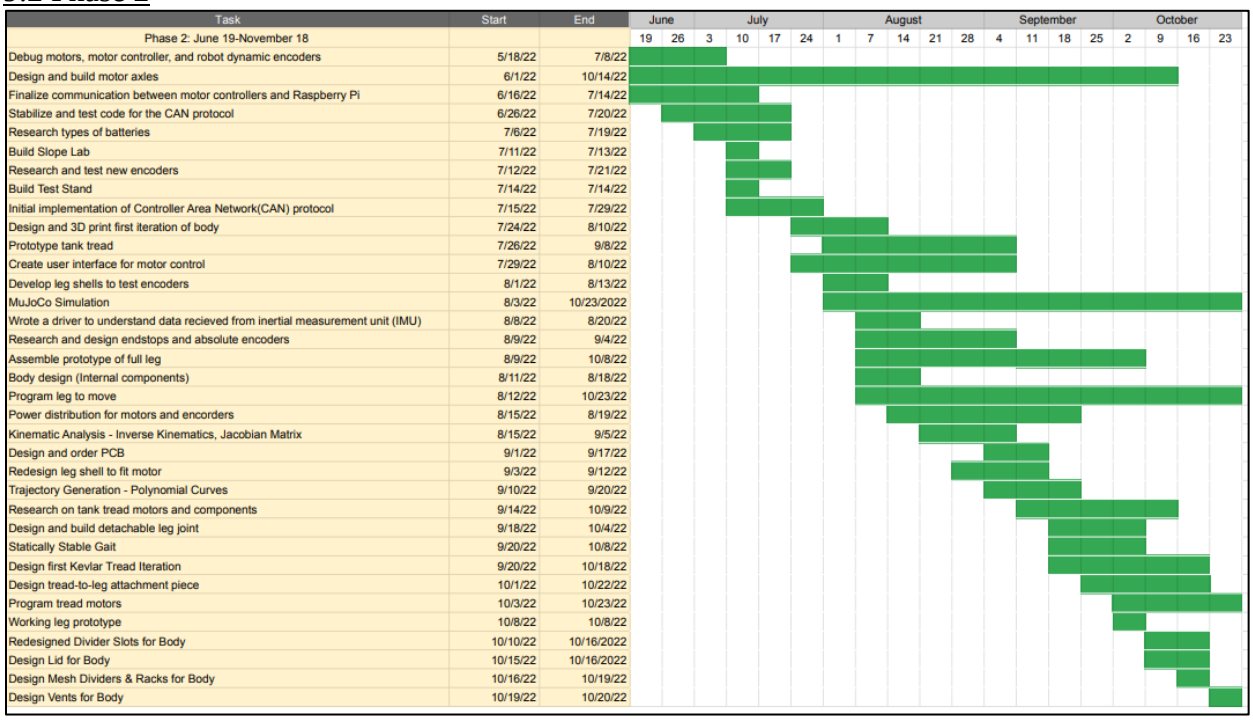

Task	Start	End
Phase 2: June 19-November 18		
Debug motors, motor controller, and robot dynamic encoders	5/18/22	7/8/22
Design and build motor axles	6/1/22	10/14/22
Finalize communication between motor controllers and Raspberry Pi	6/16/22	7/14/22
Stabilize and test code for the CAN protocol	6/26/22	7/20/22
Research types of batteries	7/6/22	7/19/22
Build Slope Lab	7/11/22	7/13/22
Research and test new encoders	7/12/22	7/21/22
Build Test Stand	7/14/22	7/14/22
Initial implementation of Controller Area Network(CAN) protocol	7/15/22	7/29/22
Design and 3D print first iteration of body	7/24/22	8/10/22
Prototype tank tread	7/26/22	9/8/22
Create user interface for motor control	7/29/22	8/10/22
Develop leg shells to test encoders	8/1/22	8/13/22
MuJoCo Simulation	8/3/22	10/23/2022
Wrote a driver to understand data recieved from inertial measurement unit (IMU)	8/8/22	8/20/22
Research and design endstops and absolute encoders	8/9/22	9/4/22
Assemble prototype of full leg	8/9/22	10/8/22
Body design (Internal components)	8/11/22	8/18/22
Program leg to move	8/12/22	10/23/22
Power distribution for motors and encorders	8/15/22	8/19/22
Kinematic Analysis - Inverse Kinematics, Jacobian Matrix	8/15/22	9/5/22
Design and order PCB	9/1/22	9/17/22
Redesign leg shell to fit motor	9/3/22	9/12/22
Trajectory Generation - Polynomial Curves	9/10/22	9/20/22
Research on tank tread motors and components	9/14/22	10/9/22
Design and build detachable leg joint	9/18/22	10/4/22
Statically Stable Gait	9/20/22	10/8/22
Design first Kevlar Tread Iteration	9/20/22	10/18/22
Design tread-to-leg attachment piece	10/1/22	10/22/22
Program tread motors	10/3/22	10/23/22
Working leg prototype	10/8/22	10/8/22
Redesigned Divider Slots for Body	10/10/22	10/16/2022
Design Lid for Body	10/15/22	10/16/2022
Design Mesh Dividers & Racks for Body	10/16/22	10/19/22
Design Vents for Body	10/19/22	10/20/22

10.0 Detailed Budget

This section details a breakdown of all expenses and funding for this project.

10.1 Phase 1 and Phase 2 Breakdown

10.1.1 Summer Interns

The following is a breakdown of five students interning a maximum of 8 weeks between June 30 and August 19, 2022. This occurs only for Phase 2.

Intern	Part/full time	Number of Weeks	Salary	Fringe	Total
1	Full-time	8	$ 5,840.00	$ 292.00	$ 6,132.00
2	Full-time	8	$ 5,840.00	$ 292.00	$ 6,132.00
3	Full-time	8	$ 5,840.00	$ 292.00	$ 6,132.00
4	Full-time	1	$ 730.00	$ 160.60	$ 890.60
5	Part-time	3	$ 1,168.00	$ 58.40	$ 1,226.40
TOTAL					$ 20,513.00

10.1.2 Forum in Pasadena, CA

A total of 17 students and one faculty advisor are traveling to Pasadena, CA for the 2022 NASA BIG Idea Challenge Forum from November 14 – 18, 2022. This occurs only for Phase 2.

Item	**Cost**
Registration	$ 9,900.00
Flights	$ 8,991.55
Hotel	$ 5,467.39
Ground transportation	$ 1,440.00
Food	$ 2,887.50
TOTAL	$ 28,686.00

10.1.3 Material Items

The following is a breakdown of material purchases for both Phase 1 and Phase 2.

Item	**Phase 1**	**Phase 2**
MSL		
Wood	$ 677.68	-
Small Supplies	$ 170.95	-
Safe Sand	$ 1,343.25	-
Prototype		
Tools	$ 1,376.61	$ 1,230.26
Tread	$ 112.67	$ 237.12
Motors	$ 1,082.23	$ 1,672.76
Raw Material and Manufacturing	$ 535.20	$ 735.00
Power Supplies and Batteries	$ 322.13	$ 614.36
Wires	$ 69.77	$ 382.73
Mechanical Components, Fasteners, Connectors	$ 365.18	$ 472.80
Computing, Sensing, and Motor Controls	$ 7,347.82	$ 458.83
Other		
Simulant soil	$ 3,675.00	-
Solder Equipment	$ 130.27	$ 829.58
Literature	$ 259.94	$ 34.55
Voltera PCB Printer	$ 4,099.98	-
Team Shirts	$ 700.00	-
UConn Indirect Costs	$ 5,636.30	$ 7,319.49
CT Space Grant Consortium Indirect Costs	-	$ 7,319.49
MSE 2023 Senior Design	-	$ 5,000.00
Total	$ 27,904.98	$ 26,306.97

10.1.4 Final Total

The final total spent by this team can be determined by the following:

10.1.1 + 10.1.2 + 10.1.3(Phase1) + 10.1.3(Phase2) = $103,410.95

10.2 Additional Funding Received

The following funds were received. Sections 10.2.1, 10.2.2, and 10.2.3 were used for travel. Section 10.2.4 was used for intern payroll.

10.2.1 ASCE Earth and Space Consortium

Five team members traveled to Denver, CO in April 2022 to give an oral presentation on this project at the ASCE Earth and Space 2022 Conference. The parentheses indicate the number of students funded per source. The funding sources and amount are as follows:

Funding Source	Total Amount
UConn Department of Materials Science and Engineering (1)	$ 1,400
UConn Department of Chemical and Biochemical Engineering (1)	$ 1,400
UConn School of Engineering Undergraduate Programs (1)	$ 1,400
UConn Department of Computer Science (1)	$ 1,400
UConn Department of Electrical Engineering (1)	$ 1,400

10.2.2 NASA Lunar Surface Innovation Consortium

Three team members will be traveling to El Paso, TX to give an oral presentation of this project at the NASA Lunar Surface innovation Consortium November 2 – 3, 2022. The parentheses indicate the number of students funded per source. The funding sources and amount are as follows:

Funding Source	Total Amount
CT Space Grant Consortium (2)	$ 3,000
UConn Department of Materials Science and Engineering (1)	$ 1,300

10.2.3 Glenn Research Center Slope Lab Testing

The UConn School of Engineering awarded this team a total of $10,000 to be used for travel to NASA Glenn Research Center for testing in the Slope Lab. This trip did not take place during the time of the 2022 NASA BIG Idea Challenge to allow the team further development of the prototype before testing in this environment. This opportunity plans to still be taken advantage of within the next year.

10.2.4 Summer Intern

The UConn Materials Science and Engineering (MSE) department funded one full-time intern to work on the project from June 30 to August 19, 2022.

Intern	Part/full time	Number of Weeks	Salary	Fringe	Total
1	Full-time	8	$ 5,980.00	$ 312.08	$ 6,292.08

11.0 Acknowledgments

The team would like to formally acknowledge the support received that allowed this project to come to fruition. Financial support and funding for this project comes from the NASA, the CT Space Grant Consortium, and University of Connecticut Department of Engineering. Support in other forms comes from Glenn Research Center, for offering a location and resources to test the rover; Collins Aerospace; Peer Robotics; and several employees from the University of Connecticut. These employees include Pete Glaude from the UConn Machine Shop, Lorri Lafontaine for materials purchasing, Tracy Mahue for travel planning and purchasing, and UConn faculty supporting students receiving credit during the Fall 2022 semester: Dr. Derek Aguiar (CSE), Dr. Ryan Cooper (ME), Dr. Fiona Leek (MSE), Dr. Rachel Tambling (HDFS).

Appendix A: References

Section 2

(1) Wilcox, K. (n.d.). *New Rover Will Examine Water Ice on the Moon*. NASA. Retrieved January 6, 2022, from https://appel.nasa.gov/2019/10/30/new-rover-will-examine-water-ice-on-the-moon/
(2) Gawronska, A.J., et al. "Geologic Context and Potential EVA Targets at the Lunar South Pole." *Advances in Space Research*, Pergamon, 15 June 2020, https://www.sciencedirect.com/science/article/pii/S0273117720303689.
(3) Chen, Guoqiang, et al. "Influence of Topography on the Site Selection of a Moon-Based Earth Observation Station." *Sensors*, MDPI, 29 Oct. 2021, https://www.ncbi.nlm.nih.gov/pmc/articles/PMC8587812/.

Section 3

(1) Costas, N. C., Farmer, J. E., & George, E. B. (1972, December). MOBILITY PERFORMANCE OF THE LUNAR ROVING VEHICLE: TERRESTRIAL STUDIES - APOLLO 15 RESULTS. Marshall Space Flight Center; NASA.
(2) DARPA. (n.d.). *Big Dog*. DARPA. Retrieved December 20, 2021, from https://www.darpa.mil/about-us/timeline/big-dog
(3) NASA. (n.d.). *Autonomous Planetary Mobility*. NASA. Retrieved December 20, 2021, from https://mars.nasa.gov/mer/mission/technology/autonomous-planetary-mobility/
(4) NASA. (n.d.). NASA BIG Idea Challenge. Retrieved December 28, 2021, from https://bigidea.nianet.org/competition-basics/
(5) NASA. (n.d.). *Reinventing the Wheel*. NASA. Retrieved December 27, 2021, from https://www.nasa.gov/specials/wheels/
(6) Orlando, A. (2020, August 16). *After Disaster Strikes, a Robot Might Save your Life*. Discover Magazine. Retrieved December 20, 2021, from https://www.discovermagazine.com/technology/after-disaster-strikes-a-robot-might-save-your- life
(7) Shen, S.-Y., Li, C.-H., Cheng, C.-C., Wang, S.-F., Lin, P.-C., & Lu, J.-C. (2009). Design of a Leg-Wheel Hybrid Mobile Platform. St. Louis; 2009 IEEE/RSJ International Conference on Intelligent Robots and Systems.

Section 4

(1) Hughes, J., Marisol, James, James, & Matthew. (2020, April 18). *Wheels vs continuous tracks: Advantages and disadvantages: Into robotics*. Into Robotics | ROS, Robots and Stuff. https://www.intorobotics.com/wheels-vs-continuous-tracks-advantages-disadvantages
(2) *AMT102-V: Digi-Key Electronics*. Digi. (n.d.). Retrieved from https://www.digikey.com/en/products/detail/cui-devices/AMT102-V/827015
(3) Cu, X. P., Vintr, Z., & Mai, D. S. (2021). Prediction of the lifetime of tank track components using the accelerated testing. *2021 International Conference on Military Technologies (ICMT)*. https://doi.org/10.1109/icmt52455.2021.9502824
(4) Hawkes, J. (2022, January 17). *Primer: Composite Rubber Track (CRT)*. Tanknology Institute. https://www.tanknology.co.uk/post/__crt
(5) AntigravityODrive. (n.d.). Retrieved from https://odriverobotics.com/
(6) MN4004 KV300 - 2PCS/set_antigravity type_motors_multirotor_t-motor store-official store for T-Motor Drone Motor,ESC,Propeller. (n.d.). https://store.tmotor.com/goods.php?id=438
(7) Parsons, R. (1970, January 1). *How to select the right power source for a hobby BLDC (PMSM) Motor*. How to select the right power source for a hobby BLDC (PMSM) motor. https://things-in-motion.blogspot.com/2018/12/how-to-select-right-power-source-for.html
(8) Roberts, C. C. (n.d.). *Failure analysis of selected fasteners used during World War II*. Roberts Armory. http://robertsarmory.com/Tank-Tracks-WW-II.pdf

(9) *Kevlar® Aramid Fiber Technical Guide - Dupont*. Dupont.com. (n.d.) https://www.dupont.com/content/dam/dupont/amer/us/en/safety/public/documents/en/Kevlar_Technical_Guide_0319.pdf
(10) *ODrive*. ODriverobotics.com. (n.d.) https://odriverobotics.com/
(11) *AN885, brushless DC (BLDC) motor fundamentals - electrathon of tampa bay*. (n.d.). from http://electrathonoftampabay.org/www/Documents/Motors/BrushlessDC(BLDC)MotorFundamentals pdf
(12) *Pulse width modulation*. Pulse Width Modulation - SparkFun Learn. (n.d.). Retrieved October 24, 2022, from https://learn.sparkfun.com/tutorials/pulse-width-modulation/all
(13) Parsons, R. (1970, January 1). *How to select the right power source for a hobby BLDC (PMSM) Motor*. How to select the right power source for a hobby BLDC (PMSM) motor. Retrieved October 24, 2022, from https://things-in-motion.blogspot.com/2018/12/how-to-select-right-power-source-for.html

Section 5

(1) *Amber-UConn*. GitHub. (n.d.). from https://github.com/AMBER-UConn
(2) AMBER-UConn. (n.d.). *Amber-uconn/amber_robot: Codebase for UConn's finalist team in the 2022 NASA Big Idea challenge. Includes robot configuration, motion control, and other tools*. GitHub. from https://github.com/AMBER-UConn/amber_robot
(3) Park, H.-W., Wensing, P. M., & Kim, S. (2017). High-speed bounding with the MIT Cheetah 2: Control Design and experiments. *The International Journal of Robotics Research*, *36*(2), 167–192. https://doi.org/10.1177/0278364917694244
(4) Zeng, X., Zhang, S., Zhang, H., Li, X., Zhou, H., & Fu, Y. (2019). Leg trajectory planning for quadruped robots with high-speed trot gait. *Applied Sciences*, *9*(7), 1508. https://doi.org/10.3390/app9071508
(5) Chen, M., Li, Q., Wang, S., Zhang, K., Chen, H., & Zhang, Y. (2021). Single-leg structural design and foot trajectory planning for a novel bioinspired quadruped robot. *Complexity*, *2021*, 1–17. https://doi.org/10.1155/2021/6627043
(6) Raheem, F. A., & Flayyih, M. K. (2019). Creeping gait analysis and simulation of a quadruped robot. *Al-Khwarizmi Engineering Journal*, *14*(2), 93–106. https://doi.org/10.22153/kej.2018.12.004
(7) Xu, K., Zi, P., & Ding, X. (2019, February 3). *Gait analysis of quadruped robot using the equivalent mechanism concept based on metamorphosis - chinese journal of mechanical engineering*. SpringerOpen. https://cjme.springeropen.com/articles/10.1186/s10033-019-0321-2#:~:text=AquadrupedrobotcanwalkˌnamedcreepinggaitsB41D.
(8) *ODrive Pro documentation*. ODrive Pro Documentation - ODrive Pro Documentation 0.6.3 documentation. (n.d.). https://docs.odriverobotics.com/v/latest/index.html
(9) *Mujoco*. MuJoCo. (n.d.).from https://mujoco.org/